

# Below-bandgap excited, terahertz emission of optically pumped GaAs/AlGaAs multiple quantum wells

Elmer Estacio<sup>a,\*</sup>, Alex Quema<sup>a</sup>, Romeric Pobre<sup>a</sup>, Gilbert Diwa<sup>a</sup>, Carlito Ponseca<sup>a</sup>, Shingo Ono<sup>a</sup>, Hidetoshi Murakami<sup>c</sup>, Armando Somintac<sup>b</sup>, Joanes Sy<sup>b</sup>, Valynn Mag-usara<sup>b</sup>, Arnel Salvador<sup>b</sup>, Nobuhiko Sarukura<sup>c</sup>

<sup>a</sup> Laser Research Center for Molecular Science, Institute for Molecular Science (IMS), 38 Nishigonaka, Myodaiji, Okazaki, Aichi 444-8585, Japan

<sup>b</sup> National Institute of Physics, University of the Philippines, Diliman, Quezon City 1101, Philippines

<sup>c</sup> Institute of Laser Engineering, Osaka University, 2-6 Yamadaoka, Suita, Osaka 565-0871, Japan

Available online 11 July 2006

## Abstract

We present terahertz (THz) emission of optically pumped 5-nm GaAs/AlGaAs multiple quantum wells (MQWs) even at excitation energies below the bandgap. The excitation energy corresponding to the peak THz emission is red-shifted with respect to the photoluminescence (PL) and photoluminescence excitation peak. This is attributed to a transient bandgap renormalization that occurs on the same time scale as the generation of the THz transients. Moreover, an emission shoulder at  $\sim 40$  meV below the THz emission peak was observed. Deep level transient spectroscopy results do not indicate that this is due to electron traps. However, an indistinct LO phonon-related, below-bandgap PL feature was seen at low temperature that coincides well with the observed THz radiation feature. It is proposed that the THz action spectrum may be sensitive to phonon-mediated processes in contrast to more conventional optical spectroscopy techniques, albeit at room temperature.

© 2006 Elsevier B.V. All rights reserved.

**Keywords:** Semiconductor; Terahertz radiation; Multiple quantum well; Longitudinal-optical (LO) phonon

## 1. Introduction

Terahertz (THz) emission spectroscopy, has over the past decade, proven to be an invaluable tool in the characterization of semiconductor heterostructures. It serves as a method for studying the dynamics of carriers under ultrafast optical excitation [1–5]. Works on the intersubband transitions, on the other hand, have led to the development of semiconductor devices operating in the THz region [6,7]. In these previous reports, the excitation energy is necessitated to be higher than the bandgap of the semiconductor to enable the creation of electron–hole (e–h) pairs. The spatial separation of e–h pairs and the surge current associated with the acceleration of these charges are among the two accepted mechanisms of THz emission in surface-irradiated semiconductors [8,9].

This work presents results on the observation of THz emission for optically excited GaAs/AlGaAs multiple quan-

tum well (MQW) heterostructures even for excitation energies below the MQW bandgap. As the THz emission contribution from the underlying bulk GaAs layer is relatively weak to account for the observed results, the emission is attributed to the two-dimensional structures themselves. The red-shifted THz emission peak is owed to a bandgap renormalization process. Furthermore, a THz emission shoulder appearing  $\sim 40$  meV below the THz peak is tentatively ascribed as possibly due to an LO phonon-assisted emission. This phonon-mediated transition was also observed by low-temperature photoluminescence (PL) spectroscopy. It is suggested that even for experiments performed at room temperature, the THz action spectrum appears to be sensitive to this type of transition compared to more conventional optical spectroscopy methods.

## 2. Experiment

The 5-nm GaAs/Al<sub>0.3</sub>Ga<sub>0.7</sub>As MQW heterostructure was grown via a Riber 32P molecular beam epitaxy (MBE) machine on a semi-insulating (carrier density  $\sim 10^{15}$  cm<sup>-3</sup>) GaAs (100)

\* Corresponding author. Tel.: +81 564 55 7477; fax: +81 564 55 7218.  
E-mail address: [estacio@ims.ac.jp](mailto:estacio@ims.ac.jp) (E. Estacio).

substrate. The structure schematics for the MQW consists of an undoped GaAs buffer layer, followed by 40 periods of 5-nm undoped GaAs QWs with undoped 10-nm AlGaAs barriers, and finally a 10 nm Si-doped ( $\sim 10^{17} \text{ cm}^{-3}$ ) GaAs cap. For the experiments, the sample was cut into a 2 mm  $\times$  2 mm piece. Initially, PL spectroscopy measurements were performed using an Ar<sup>+</sup> laser ( $\lambda_e = 488 \text{ nm}$ ) as excitation and a 0.5 m spectrometer fitted with a GaAs photomultiplier to disperse and detect the PL signal, respectively. This was done to probe the band structure and to assess the quality of the layers. The THz emission experiments were carried out using a mode-locked, 100 fs-pulsed (86 MHz repetition rate) Ti: sapphire laser as the excitation. The laser was tuned from 1.38 to 1.55 eV (900–800 nm) at 10 meV increments to obtain the THz action spectrum. All throughout the experiment, the spectral width, beam-spot diameter, and the optical power of the laser were maintained at 20 meV,  $\sim 1 \text{ mm}$ , and 160 mW, respectively. The broadband THz radiation power was collected, collimated and focused onto a liquid He-cooled Ge bolometer using paraboloidal mirrors. For selected excitation energies, the time domain spectroscopy (TDS) spectra for the MQWs were taken using a low temperature-grown GaAs photoconductive antenna. In conjunction with this, room temperature photoluminescence excitation (PLE) measurements using the same optical excitation parameters, a suitable band-pass filter, and silicon photodiode was performed. To determine the presence of electron traps, the MQW layer underwent deep level transient spectroscopy (DLTS). The sample was fabricated into arrays of 250  $\mu\text{m}$ -diameter circular mesas using standard photolithography techniques. The bottom and the top indium contacts were then deposited via thermal evaporation. Temperature scans were performed from 77 to 370 K. To generate the Arrhenius plots and to ascertain the activation energy of the traps, four frequency scans (10 Hz, 100 Hz, 500 Hz and 1 kHz) were also performed with a reverse bias of  $-6 \text{ V}$  and a filling pulse of 1 V. Finally, PL spectroscopy at 10 K was done to verify the presence of below-bandgap optical transitions.

### 3. Results and discussion

For semiconductors excited by femtosecond optical pulses with energy higher than the bandgap, transient e–h pairs are initially created, separating in a picosecond timescale. This transient e–h dipole radiates a picosecond pulse with frequencies spanning 0.1 THz to about 2 THz. Secondly, the carriers are accelerated by the surface depletion field, emitting electromagnetic (EM) radiation in the THz range [10]. In the far field, the EM wave is proportional to the time derivative of the current,  $\partial j/\partial t$ . The current,  $J$ , may be expressed as  $J = Nev$ , where  $N$ ,  $e$ , and  $v$  are the number of photogenerated carriers, the elementary electric charge, and the carrier velocity, respectively. In MQW's, where the surface field may well extend to the quantum well region, this is the current  $J$  flowing across the heterostructures, as in the bulk semiconductor case [9].

Shown in Fig. 1(a) is the THz action spectrum of the MQW sample. Primarily, it is expected that the energetic location of the THz radiation power peak should coincide with the MQW

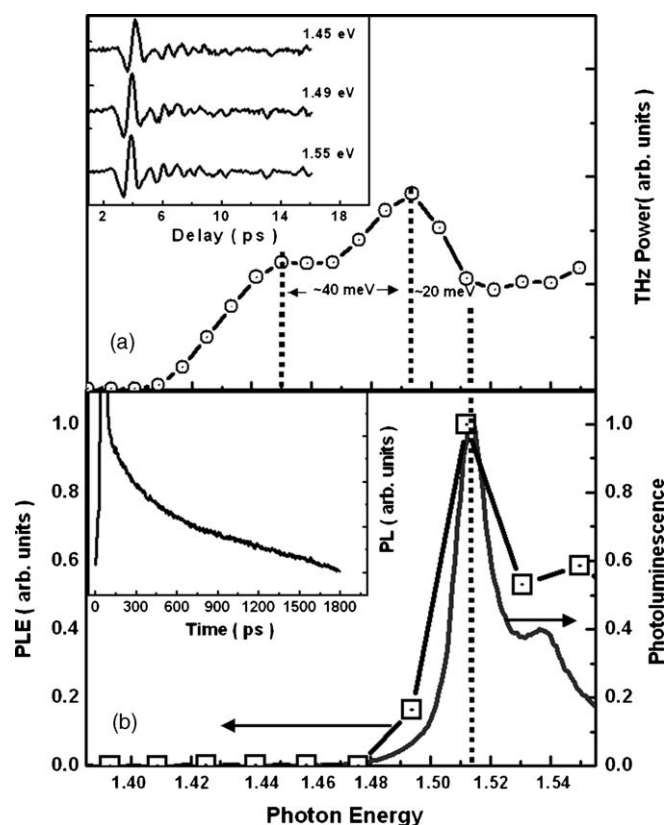


Fig. 1. (a) The THz action spectrum of the 5 nm MQW sample. The THz emission peak occurs at excitation energy, 20 meV below the bandgap. This is attributed to transient bandgap renormalization. A spectral feature at 1.45 eV is tentatively ascribed to an LO phonon-mediated transition. The inset compares the lineshapes of the TDS spectra for selected excitation energies where no apparent variation in the THz radiation mechanism is seen for each case. (b) The corresponding PL and PLE spectra showing good agreement with the expected bandgap value. The inset shows the decay time of the PL signal. This confirms that for a laser repetition rate of  $\sim 86 \text{ MHz}$ , no excess carriers will persist; hence, the absence of long term bandgap shrinkage.

bandgap where maximum photocarrier absorption occurs. The observed THz emission peak instead sits at 20 meV below the calculated bandgap using effective mass approximation methods [11]. This is attributed to a transient bandgap renormalization process [12]. No excitation fluence dependence studies have been done but at this excitation condition, we expect carrier density-dependent shrinkage of the bandgap to occur (photocarrier density is estimated to be of the order of  $10^{17} \text{ cm}^{-3}$  at 1.45 eV excitation) [13]. Furthermore, a THz emission shoulder appeared at an excitation energy  $\sim 40 \text{ meV}$  below the observed THz emission peak. The origin of this feature will be discussed in more detail later in the text. The TDS spectra for selected excitation energies are shown in the inset to compare the lineshapes of the TDS features. The TDS trace for each excitation energy was offset and re-scaled for ease-of-comparison. Aside from the slight delay of the 1.45 eV trace, the lineshapes of the spectra did not appear to vary. This indicates that as far as the detection bandwidth ( $\sim 2 \text{ THz}$ ) of the TDS setup is concerned, the THz radiation mechanism attributed to the transient current from the e–h dipole was dominant for excitation energies both below and above the MQW bandgap. Consequently, the observed THz radi-

ation may be ascribed to the generated photocarriers in the MQW structures for the entire region of the THz action spectrum.

The room temperature PL and PLE spectra agreed well with the calculated bandgap energy and no below-bandgap features were observed as shown in Fig. 1b even though the PLE spectrum was taken using the same optical excitation conditions as in the THz action spectrum. Apparently, no bandgap renormalization was observed in the luminescence measurements. This is explained by considering the difference in the mechanism of photoluminescence and of the THz transient generation. While the THz transients are caused by the current surge from the e–h dipole, the luminescence is only observed after the photogenerated electrons have recombined with the holes. This indicates that the two mechanisms occur at different temporal regions. The inset in Fig. 1b shows the time-resolved PL of the MQW sample at room temperature. Clearly, the PL signal persists up to 1200 ps. Relating this data to the PLE spectrum, the time-integrated PLE photodiode-signal did not exhibit the transient bandgap renormalization occurring at a much earlier time when the photocarrier density is large. In addition, no long-term renormalization is observed since no excess carriers persist in the MQW's. With a repetition rate of  $\sim 86$  MHz, the PL signal has long decayed before the next optical pulse arrives after  $\sim 11$  ns. In contrast to the luminescence, the THz signal due to the transient current disappears after  $\sim 6$  ps as per the TDS data. This THz transient generation occurs during the time-scale associated with transient bandgap renormalization. The transient bandgap renormalization and recovery has been reported previously for both bulk and quantum well layers and is not extraordinary [14,15].

To ascertain that the THz radiation indeed originated from the two-dimensional structures and not from the underlying bulk GaAs layers, the THz action spectra for semi-insulating and n-type GaAs wafers were taken and are compared with the MQW sample in Fig. 2. The observed THz radiation power of the bulk GaAs wafers is significantly less intense. For the n-type GaAs

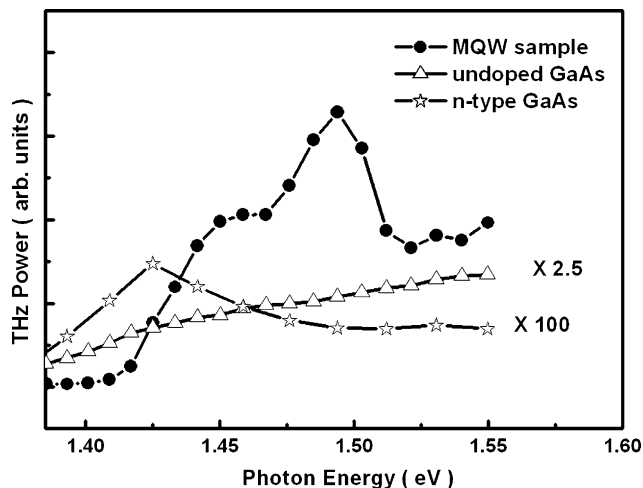


Fig. 2. A comparison of the relative intensity of the THz action spectra for the MQW sample and bulk GaAs wafers. The comparably low THz power from the bulk wafers lends proof that the dominant THz radiation from the sample originated from the MQW structures and not from the GaAs cap or the underlying bulk GaAs buffer layer.

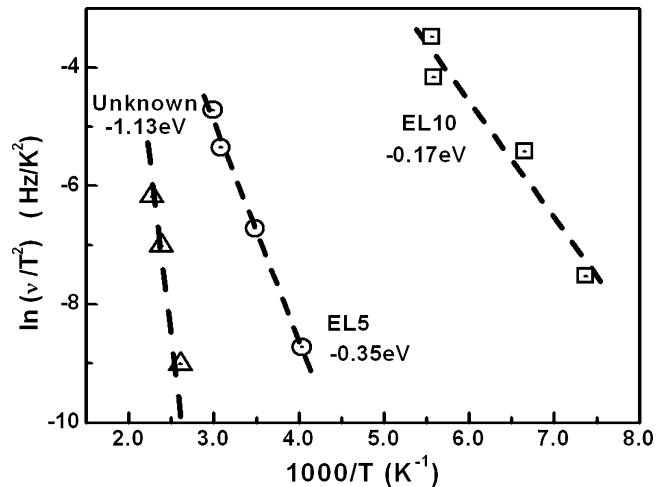


Fig. 3. Arrhenius plots that were derived from DLTS data showing three types of traps. The calculated activation energies of the traps are not in the range of the observed below-bandgap excited THz emission. As such, the below-bandgap excitation feature is attributed to a different phenomenon.

sample, THz radiation power was two orders of magnitude less than the MQW sample. Taking the comparatively thin n-type GaAs cap layer (10 nm) of the MQW into consideration, contribution from the cap region should therefore be insignificant. The radiation from the undoped GaAs wafer was less than 2.5 times that of the MQW's. However, considering the enhanced absorption coefficient of the MQW heterostructures due to quantum confinement, the estimated optical excitation power reaching the underlying bulk layer is only  $\sim 15\%$  of the incident. Thus, it is expected that the contribution from the bulk GaAs region under the MQW heterostructures should be less than 10% of the total detected THz power. As a consequence, the observed THz action spectrum of the MQW sample may be safely ascribed to the photocarriers from the GaAs/AlGaAs MQW structures.

The presence of deep level traps that may have been incorporated during the growth process was initially surmised to cause the THz emission peak at an excitation energy  $\sim 40$  meV below the THz emission maximum. As shown in Fig. 3, results of the DLTS experiment revealed the presence of three types of traps; EL5, EL10, and an unidentified trap. The EL5 trap is attributed to Ga vacancies or a complex defect of  $\text{As}_{\text{Ga}}$  [16,17]. The EL10 trap is a low-energy GaAs trap described by Martin et al. [18]. In addition, the deep levels of a bare GaAs substrate is also studied and it is ascertained that the DLTS signals came from the MBE-grown layers and not from the substrate itself. The activation energy of the traps, however, could not account for the energetic location of the below-bandgap THz emission. To further assess the optical contribution from these traps, PL spectroscopy was performed at 10 K. Shown in Fig. 4 is the PL peak associated with the 1st conduction band-to-1st heavy-hole band transition. This is in good agreement with 10 K bandgap of the heterostructure. However, no distinguishable below-bandgap PL features were observed. A higher resolution PL scan was performed on the low energy side of the main PL peak and is shown in the inset of Fig. 4. The log plot revealed an indistinct PL feature at an energy,  $\sim 37$  meV below the excitonic

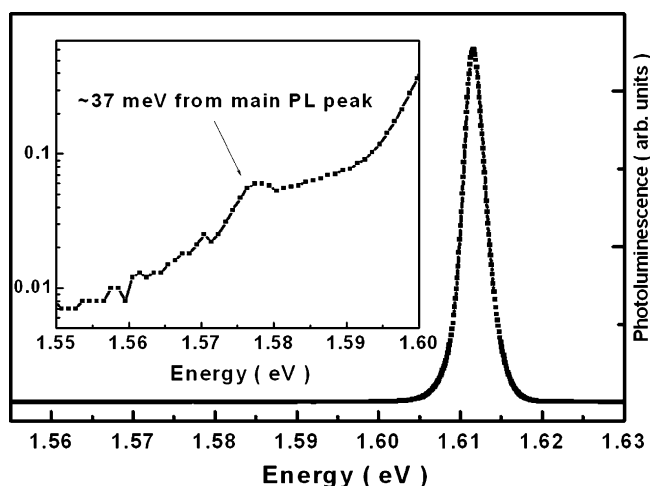


Fig. 4. Low temperature PL spectrum of the MQW layer. The inset shows an indistinct luminescence feature at  $\sim 37$  meV below the bandgap for a higher-resolution PL scan. This is owed to an LO phonon-mediated transition and incidentally coincides well with the  $\sim 40$  meV red-shifted feature in the THz action spectrum.

emission peak. This is attributed to an LO phonon-assisted PL emission [19]. A phonon-mediated process such as this is not easily observed especially in room temperature optical measurements. Incidentally, this red-shifted PL feature coincides well with the  $\sim 40$  meV below-bandgap excitation feature that was observed in the THz action spectrum. With the premise that the THz radiation mechanism is dominated by the surge current from the photogenerated e–h dipole and that no defect-related traps could account for the  $\sim 40$  meV red-shifted feature, the LO phonon-mediated process is proposed as the origin of this feature in the THz action spectrum of the MQW. Consequently, the data imply that THz spectroscopy appears to be more sensitive to phonon-assisted processes compared to more conventional optical spectroscopy techniques. Although further experiments such as temperature-dependent THz spectroscopy can be performed to verify the contribution of phonon-related processes, the observation is tentatively attributed to an LO phonon-assisted transition.

#### 4. Summary

In summary, the THz action spectrum of a 5 nm GaAs/AlGaAs MQW sample exhibited emission even for excitation energies below the bandgap. Primarily, the pump energy corresponding to the THz emission peak is red-shifted by 20 meV as compared to the PL and PLE experiment. This is attributed to a transient bandgap renormalization process that was not detected by the time-integrated PL and PLE experiments. Furthermore, the appearance of a THz emission feature at  $\sim 40$  meV below the THz radiation peak is suggested to be due to an LO phonon-mediated transition in the MQW structure. This transition was also observed using low-temperature PL spectroscopy. Further

investigation may be required to verify this suggestion but the present results imply that even for experiments performed at room temperature, the THz action spectrum of the MQW sample may be sensitive to an LO phonon-assisted optical process.

#### Acknowledgements

This research was partially supported by a Grant-in-Aid for JSPS Fellows (16-04077) from Japan Society for the Promotion of Science (JSPS), a Grant-in-Aid for Creative Scientific Research, a Grant-in-Aid for Scientific Research on Priority Areas (16032216), a Grant-in-Aid for Creative Scientific Research Collaboration on Electron Correlation (13NP0201), a Grant-in-Aid for Young Scientists (B) (16760043) and Special Coordination Funds for Promoting Science and Aid Technology from the Ministry of Education, Culture, Sports, Science and Technology (MEXT). A. Salvador thanks DOST-PCASTRD for the research grant. Acknowledgment is also given to C. Ison and M. Bailon, and J. Mateo for their invaluable contributions to this work.

#### References

- [1] P. Planken, M. Nuss, I. Brener, K. Goosen, M. Luo, S. Chuang, L. Pfeiffer, *Phys. Rev. Lett.* 69 (1992) 3800–3803.
- [2] J. Cerne, J. Kono, M. Sundaram, A. Gossard, G. Bauer, *Phys. Rev. Lett.* 77 (1996) 1131–1134.
- [3] N. Sekine, K. Hirakawa, M. Voßbürger, P. Haring Bolivar, H. Kurz, *Phys. Rev. Lett.* 64 (2001) 201323-1–201323-4.
- [4] T. Liu, K. Huang, C. Pan, S. Ono, H. Ohtake, N. Sarukura, *Jpn. J. Appl. Phys.* 40 (2001) L681–L683.
- [5] I. Morohashi, K. Komori, S. Wang, T. Hidaka, M. Ogura, M. Watanabe, *Jpn. J. Appl. Phys.* 40 (2001) L681–L683.
- [6] A. Maslov, D. Citrin, *J. Appl. Phys.* 93 (2003) 10131–10133.
- [7] H. Liu, C. Song, A. SpringThorpe, J. Cao, *Appl. Phys. Lett.* 84 (2004) 4068–4070.
- [8] S. Chuang, S. Schmitt-Rink, B. Greene, P. Saeta, A. Levi, *Phys. Rev. Lett.* 68 (102) (1992).
- [9] Y. Kadoya, K. Hirakawa, in: K. Sakai (Ed.), *Terahertz Optoelectronics, Topics in Applied Physics*, vol. 97, Springer-Verlag, Berlin, Heidelberg, 2005, pp. 117–118.
- [10] C. Weiss, R. Wallenstein, R. Beigang, *Appl. Phys. Lett.* 77 (4160) (2000).
- [11] F. Pollak, in: P. Bhattacharya (Ed.), *Properties of III–V Quantum Wells and Superlattices*, EMIS Data Reviews Series, vol. 15, INSPEC, England, 1996, pp. 232–240.
- [12] S. Schmitt-Rink, D.S. Chemla, D.A.B. Miller, *Adv. Phys.* 38 (1989) 89–188.
- [13] H. Haug, S. Koch, *Phys. Rev. A* 39 (2003) 1887–1898.
- [14] P.W. Juodawlskis, S.E. Ralph, *Appl. Phys. Lett.* 76 (2000) 1722–1724.
- [15] H. Roskos, B. Rieck, A. Seilmeier, W. Kaiser, G.G. Baumann, *Phys. Rev. B* 40 (1989) 1396–1399.
- [16] H. Shiraki, Y. Tokuda, K. Sassa, *J. Appl. Phys.* 84 (1998) 3167–3174.
- [17] K. Yokota, H. Kuchii, K. Nakamura, M. Sakaguchi, Y. Ando, *J. Appl. Phys.* 88 (2000) 5017–5021.
- [18] G. Martin, A. Mittonneau, A. Mircea, *Electron. Lett.* 13 (1977) 191–193.
- [19] B.V. Shanabrook, S. Rudin, T.L. Reinecke, W. Tseng, P. Newman, *Phys. Rev. B* 17 (1990) 1577–1580.